

# Mechanism Analysis of Interrupted Growth of Single-Walled Carbon Nanotube Arrays

Takayuki Iwasaki,<sup>†</sup> John Robertson,<sup>‡</sup> and Hiroshi Kawarada<sup>\*†</sup>

*Department of Electronic and Photonic Systems, Waseda University, 3-4-1 Ohkubo, Shinjuku-ku, Tokyo 169-8555, Japan, and Department of Engineering, University of Cambridge, Cambridge CB2 1PZ, United Kingdom*

*Received November 29, 2007; Revised Manuscript Received January 7, 2008*

## ABSTRACT

We investigated the growth mechanism of layered single-walled carbon nanotube (SWNT) mats by a cutting method. Transmission electron microscope observations revealed that new SWNTs grown below first grown SWNTs also have caps at their tips. Raman spectroscopy suggests that the SWNTs in each layer have the same chirality distribution. This growth method might be a way to prove a factor of chirality selection of SWNTs.

Carbon nanotubes (CNTs) have been intensively studied because of their unique structural and electronic properties. CNTs are candidates for practical applications such as transistors,<sup>1</sup> field emitters, LSI interconnects,<sup>2,3</sup> and capacitors.<sup>4,5</sup> There is particular interest in nanotubes grown as vertically aligned mats, both multi-walled carbon nanotubes (MWNTs)<sup>6–10</sup> and single-walled carbon nanotubes (SWNTs)<sup>11–16</sup> fabricated by various chemical vapor deposition (CVD) methods. Some of these applications require either semiconducting or metallic SWNTs, which depends on the  $(n, m)$  chiral index or wrapping vector of the nanotube. There are methods to separate the nanotube types after growth,<sup>17,18</sup> but they are costly and time-consuming. It would be preferable to be able to grow a particular type or chirality. However, this has also been problematic. So far, it has only been possible to grow a narrow range of chiralities by CVD because tubes of different chiralities have only a small free energy difference.

Nanotubes are known to grow by one of two growth mechanisms, root- or tip-growth, depending on whether the nanotube grows from the catalyst at its root or tip. Smalley et al.<sup>19,20</sup> suggested that a way to produce a nanotube mat of single chirality is by “cloning”: to form a mat of previously separated nanotubes and to continue the growth of the nanotubes by tip growth after “docking” catalyst atoms on their tips. Here we demonstrate another means to produce continued growth while retaining chirality distribution, but in the root growth mechanism, which is the prevalent growth

mechanism of SWNT mats. In addition, we show that this growth method may prove a factor of chirality selection of SWNTs.

The layer or marker method was recently used to determine the growth mode of SWNT and MWNT mats in CVD.<sup>21–24</sup> This consists of interrupting the nanotube growth by lowering the substrate temperature and/or turning off the plasma, according to some time sequence, and observing layering of the resulting stack. Growth interruptions produce clear interfaces. In Figure 1c, it is clear that root growth occurred because the bottom layer corresponds to the last, short time growth.

The continued growth experiment raises the question, how does growth restart? It was found to be possible to separate the layers at the interface formed by interrupted growth by cutting by a razor blade. This indicates a weak adhesion between the layers. This revealed the top surface of the second, lower layer, which was then characterized. The top surface of the lower layer was found to possess caps, showing that it regrew just like a fresh layer, and many selected area Raman spectra show that the chirality distribution of the two layers is the same across the interface despite new caps being formed.

Our vertically aligned SWNTs and double-walled carbon nanotubes (DWNTs) were grown by a remote plasma CVD method on Si wafers using a sandwich-like structure catalyst of 0.5 nm  $\text{Al}_2\text{O}_3$ /0.3–0.5 nm Fe/5 nm  $\text{Al}_2\text{O}_3$ . The CVD system and catalyst preparation are described in detail elsewhere.<sup>21</sup>

Layered growth of SWNTs was performed as follows. First, a substrate with a catalyst was preheated at 600 °C for

\* Corresponding author. E-mail: kawarada@waseda.jp. Telephone: +81-3-5286-3391. Fax: +81-3-5286-3391.

<sup>†</sup> Department of Electronic and Photonic Systems, Waseda University.

<sup>‡</sup> Department of Engineering, University of Cambridge.

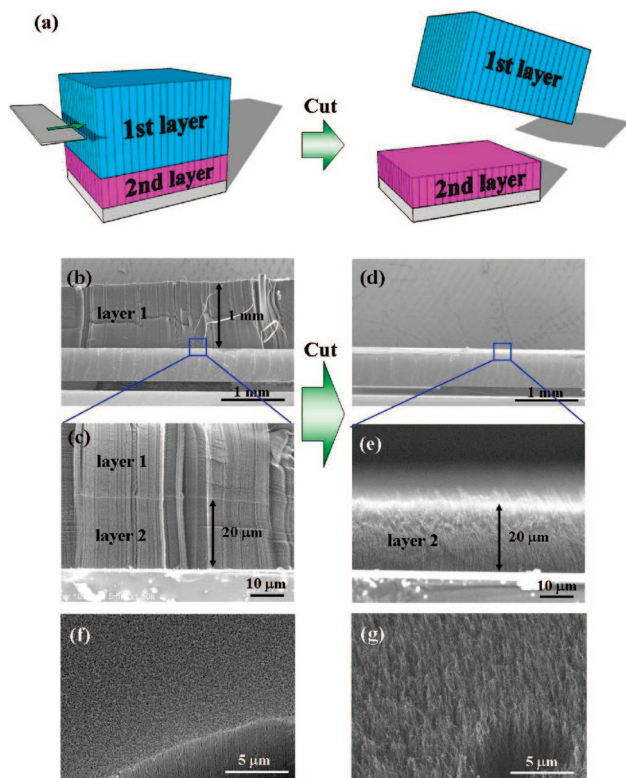


**Figure 1.** Cutting of layered SWNTs. (a) Schematic of the cutting procedure using a razor blade. (b,c) Double-layered vertically aligned SWNTs before cutting. Length of the layer 1 was on the order of a millimeter for hand cutting. (d,e) The sample after cutting. Only layer 2 was left on the substrate. The top surface of (f) layer 1 and (g) layer 2.

5 min to convert the Fe film into catalyst nanoparticles. Then a microwave power of 60 W was applied in a mixture of  $H_2$  and  $CH_4$  gases. The flow rates of  $H_2$  and  $CH_4$  were 45 and 5 sccm, respectively, and the total pressure was 20 Torr. The first layer of SWNTs was grown for 1–5 h, as mats several hundred micrometers high are needed for cutting. The growth rate was about 200–300  $\mu\text{m}/\text{h}$ . Then the heater and plasma were switched off and the sample was cooled for 5–30 min, after which the substrate was heated to 600  $^\circ\text{C}$  and the plasma restarted for growth of the second layer. This procedure was repeated for more stacks. To make DWNTs, the preheating temperature was raised to 640  $^\circ\text{C}$  to obtain the appropriate particle size.<sup>25</sup> The other conditions were the same as that for SWNT growth.

The resulting nanotubes were characterized by field emission scanning electron microscopy (FE-SEM), transmission electron microscopy (TEM), and micro-Raman spectroscopy. The Raman spectra were measured by using 514 and 633 nm excitation lasers from cross-sections of each layer with a 50 $\times$  objective lens so the area resolution was a few micrometers.

Parts b and c of Figure 1 show an SEM image of a double-layered mat. Although layer 2 grew last, it lies below layer 1 because of the root growth mode.<sup>21</sup> Figure 1c also shows the interface between layers 1 and 2, with apparently continuous bundles across the interface.

The layers were separated by applying a lateral force by a razor blade lightly and slowly to the upper layer, as shown

in Figure 1a. The samples were stuck on glass slides or Si substrates with double-sided tape. The upper layer would peel off easily, indicating that adhesion at the interface is surprisingly weak. This means that the nanotubes may not be continuous across the interface. Parts d and e of Figure 1 show the sample after cutting layer 1. Only layer 2 was left on the substrate.

Hand cutting is possible because the upper layers are quite thick,  $\sim 1$  mm.<sup>26</sup> The cutting process could be optimized; applying a slicing action from opposite sides produced a better separation. The top surface of layer 2 has an interesting structure. Parts f and g of Figure 1 show surfaces of layer 1 before cutting and layer 2 after cutting. It is well-known that the top surface of CNTs with small diameters such as SWNTs and DWNTs are curved due to a low density of CNTs at the initial growth stage.<sup>16</sup> On the other hand, as shown in Figure 1g, the top surface of layer 2 shows a sharper structure, resulting from an almost uniform length of layer 2 SWNTs.

The nanotube tips of each layer were examined by TEM. Parts a and b of Figure 2 show tips of a SWNT and a DWNT in the top layer. Both tips have a cap, and no catalyst particles were observed. This is typical for root growth.<sup>27,28</sup> Parts c and d of Figure 2 show that tips of a SWNT and a DWNT in layer 2 also have a cap. This is a key observation, as it shows that regrowth of layer 2 started with new caps, not by continuing the previous tubes.

Raman measurements were used to measure the diameter and chirality distribution of the SWNTs in each layer. Figure 3 shows the low frequency radial breathing modes (RBMs) of layers 1 and 2 for two samples that were grown in different CVD runs, and the top panel shows a Kataura plot as a function of nanotube diameter and wavenumber.<sup>29</sup> The RBM wavenumber is inversely proportional to the nanotube diameter. We see that the Raman spectra of layers 1 and 2 for each sample show almost the same RBM peaks (peak position and relative intensity), while the detailed peak distribution is different for the two samples.

RBMs of particular nanotube chiralities have a high intensity when their sub-band gaps are resonant with the excitation wavelength. This allows the nanotube chiralities to be indexed from their RBM peaks.<sup>30,31</sup> We see that nanotubes in layers 1 and 2 show almost the same peaks in their RBM peaks in Figure 3. Although the two samples show different RBM peaks, especially for 633 nm excitation, the relative intensities in each sample are preserved after growth of layer 2. This suggests that the two SWNT mats have the same diameter and chirality distribution in each layer.

We have three observations: (1) there is weak adhesion across the interface, (2) new tips occur when growth restarts, and (3) the diameter and chirality distribution appears to be continuous across the interface. A possible growth mechanism to account for these factors is shown in Figure 2e. The catalyst exists as a series of nanoparticles on the support. First, a carbon cap nucleates on each catalyst nanoparticle surface, perhaps anchored at its step edges. This cap then grows into a SWNT in layer 1. When layer 1 growth is

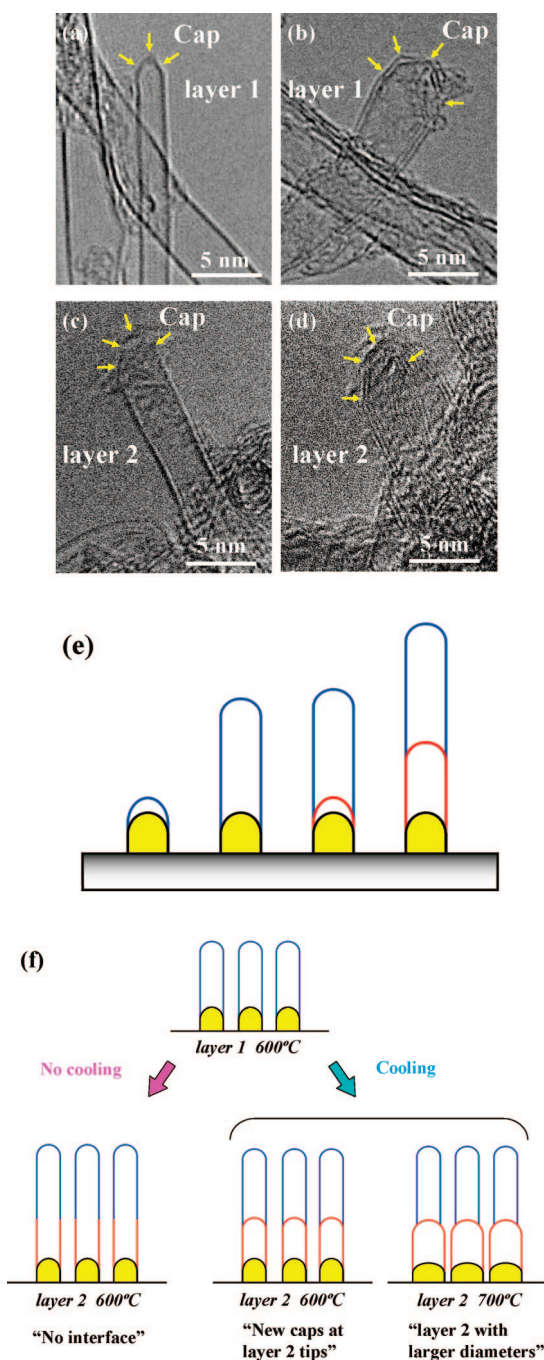


**Figure 2.** Investigation of mechanism of layered growth. TEM images of tip structures of (a) first SWNT, (b) first DWNT, (c) second SWNT, and (d) second DWNT. (e) Schematic of the growth mechanism of layered SWNTs. (f) Layered growth of SWNT mats under different conditions.

interrupted, growth restarts by forming a new cap, which then grows into a tube of layer 2. Because the new cap grows from the same catalyst nanoparticle, which is solid, it can have the same diameter as the first cap. The interface between the new cap and the old tube is not so strong and may be bound by van der Waals forces. This accounts for the rather weak adhesion across the interface.

On restarting growth, why do new carbon atoms form a new cap instead of simply continuing the growth of the previous nanotube? The answer is that cooling the system

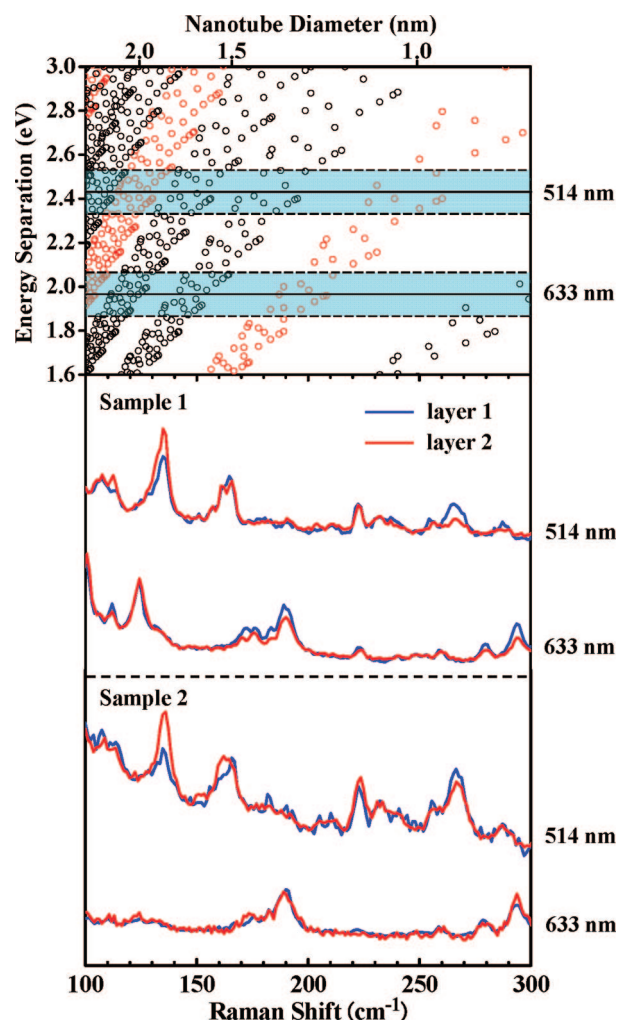


**Figure 3.** RBM peaks in Raman spectra of layers 1 and 2. Raman spectra were measured using 514 and 633 nm excitation lasers. Samples 1 and 2 were grown in different CVD runs. The top graph shows a Kataura plot as a function of nanotube diameter and wavenumber. Black and red circles indicate semiconducting and metallic nanotubes, respectively.

causes a carbon supersaturation within the catalyst nanoparticle. On reheating, this carbon rapidly emerges from the catalyst and precipitates as a new cap.<sup>32–34</sup> SWNTs can only form when there is a moderate, continuous supply of carbon, not an oversupply.

At an atomic level, a new cap forms if a graphitic cap is forced to form by rapid precipitation of carbon. This breaks the normal C–Fe bonds anchoring the cap to the catalyst surface. If the temperature is not reduced, the C–Fe bonds are retained and new C atoms can be continuously added to the root of the growing nanotube without forming a new cap. The new cap is somewhat analogous to the bamboo structure that can form in MWNTs.

To show the importance of the cooling on formation of layer 2, we tried interrupting growth by switching off the plasma but without cooling. (Note that a plasma is needed for growth in our system under normal conditions because the source gas is methane.) Several CVD runs using many substrates were performed, and no distinct interface was observed for any samples. During the interval, a catalyst



remains saturated with carbon but not oversaturated. In this case, we assume that new carbon atoms of layer 2 precipitate directly on the edge of the existing SWNTs and continuous SWNTs are grown. It is interesting to know how small a temperature change is possible before separation of the layers occurs. In our case, there might be a slight temperature change between plasma on and off although the nearly perfect remote plasma condition, in which there is no measurable ion current to the substrate, is obtained. However, this change does not produce the separation. Necessary cooling temperature will be clarified in future studies by performing experiments with different temperatures during the interval between growth of the layers.

The effects of rapid temperature changes on the cluster shape can be considered. For in situ heating up to 700 °C and cooling of a catalyst with an as-grown SWNT, Zhu et. al.<sup>27</sup> found that the catalyst shape and crystallinity were retained. Thus, the heating for the second growth stage will not affect the catalyst shape when the same temperature is used. As a result, the second SWNT has the same diameter as the first one even though they are not continuous. Repeating cooling, heating, cap formation, and SWNT growth should not change the catalyst cluster shape and crystal phase, and SWNTs with the same diameter can be synthesized on one cluster.

SWNTs with different diameters grow at higher temperatures. When the growth temperature is increased from 600 to ~700 °C for layer 2 growth, the diameter distribution of SWNTs shifts to a large diameter,<sup>21</sup> so that SWNTs grow with different diameters. It is assumed that catalyst nanoparticles have expanded slightly at the high temperature. This indicates that diameter and chirality control is possible only at low temperatures if the shape and steps of the catalyst nanoparticles are sufficiently well controlled.

We summarize the growth of layered SWNT mats under different conditions in Figure 2f. No interfaces were observed if samples were not cooled after the first SWNT growth. Interfaces were formed only if the sample was cooled after the first growth. Although new caps were formed at the tips of the layer 2 SWNTs, SWNTs of both layers grown at the same temperature had the same chirality distribution. The two SWNTs are attached by van der Waals attractions so the layer 1 SWNTs can be easily peeled off from layer 2. If the growth temperature for the second growth increased, newly grown SWNTs had larger diameters and different chiralities, probably due to reshaping of catalyst clusters at the higher temperature.

It is interesting to consider the growth mechanism in more detail. How do the layer 2 SWNTs have the same chirality distribution as those of layer 1? There are two possibilities, as shown in Figure 4. Figure 4a shows SWNTs with an identical chirality on a catalyst with a specific crystal phase. This is the principle of epitaxial control of nanotube growth.<sup>27,28</sup> Thus, each particle could create two nanotubes of the same chirality. The catalyst is solid under our conditions, as recently demonstrated by in situ studies.<sup>35,36</sup> The nanotubes grow by a vapor–solid–solid (VSS) mechanism. It is known that the cap structure determines the

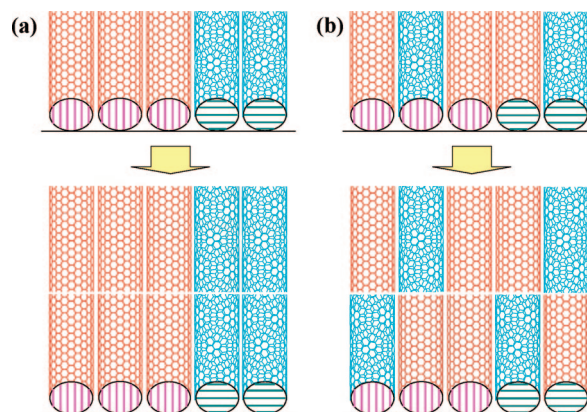


**Figure 4.** Possible combinations of nanotubes with different chiralities but the same diameter, and catalysts with different crystal phases in two layers. Catalysts with vertical or horizontal stripes have different crystal phases but have the same diameter. (a) Epitaxial growth of SWNTs. (b) SWNT growth independent with a catalyst crystal phase, but the ratio of specific chiralities is determined by the growth environment. Pictures of nanotubes were drawn by software developed by Maruyama.<sup>37</sup>

chirality of a SWNT. The cap formation strongly depends on shape and crystallinity of the nanoparticle, probably in particular, a step-edge structure, which acts as the cap nucleation site. When two SWNTs grow on the same step-edge of a nanoparticle, they should have the same chirality.

Another possibility is that SWNTs grow independently of the crystal phase of nanoparticles, as shown in Figure 4b. In this case, some SWNTs in layer 2 have different chirality from layer 1 and chirality is not continuous across the interface. However, the two layers should have the same chirality distribution as their Raman RBM peaks show almost the same relative intensities. In this case, we speculate that the ratio of SWNTs with specific chiralities would be determined by growth environment such as temperature, pressure, and feedstock. This occurs because tubes of different chiralities have only a small free energy difference.

The diameter of DWNTs is not easily evaluated as SWNTs because their outer wall diameters (4–5 nm) are below the range of normal RBM peaks. However, considering results of the TEM observations, which were similar with SWNTs, it is expected that DWNTs in layers 1 and 2 have the same diameter and chirality distribution.

In conclusion, we investigated the mechanism of layered SWNTs by cutting with a razor blade and found that new caps were formed when growth restarted. Raman spectra revealed that the two layers grown at the same temperature on the set of catalyst particles have almost the same chirality distribution. Regrowth at a higher temperature caused different diameters of layer 2 SWNTs. The diameter and chirality have been preserved in the layer 2 growth, even after the first process has been terminated when the physical conditions were kept as same as before. Two possible modes are proposed. The first one is simply explained by epitaxial regrowth of SWNTs from an oriented and immobile catalyst particle. The second one is that physical conditions determine the distribution of chirality of SWNTs according to the subtle difference in free energy of chiralities. In this case, irrespec-

tive of orientation of catalyst particle, similar chirality distribution can be reproduced if the size of particles is fixed.

**Acknowledgment.** This research was partially supported by the MIRAI project by NEDO and by “Ambient SoC Global COE Program of Waseda University” of the Ministry of Education, Culture, Sports, Science and Technology, Japan.

## References

- (1) Javey, A.; Guo, J.; Farmer, D. B.; Wang, Q.; Wang, D.; Gordon, R. G.; Lundstrom, M.; Dai, H. *Nano Lett.* **2004**, *4*, 447.
- (2) Nihei, M.; Haribe, M.; Kawabata, A.; Awano, Y. *Jpn. J. Appl. Phys.* **2004**, *43*, 1856.
- (3) Duesberg, G. S.; Graham, A. P.; Kreupl, F.; Liebau, M.; Seidel, R.; Unger, E.; Hoenlein, W. *Diam. Relat. Mater.* **2004**, *13*, 354.
- (4) Li, J.; Cassell, A.; Delzeit, L.; Han, J.; Meyyappan, M. *J. Phys. Chem. B* **2002**, *106*, 9299.
- (5) Futaba, D. N.; Hata, K.; Yamada, T.; Hiraoka, T.; Hayamizu, Y.; Kakudate, Y.; Tanaike, O.; Hatori, H.; Yumura, M.; Iijima, S. *Nat. Mater.* **2006**, *5*, 987.
- (6) Fan, S.; Chapline, M. G.; Franklin, N. R.; Tomblor, T. W.; Cassell, A. M.; Dai, H. *Science* **1999**, *283*, 512.
- (7) Cassell, A. M.; Verma, S.; Delzeit, L.; Meyyappan, M.; Han, J. *Langmuir* **2001**, *17*, 260.
- (8) Merkulov, V. I.; Melechko, A. V.; Guillorn, M. A.; Lowndes, D. H.; Simpson, M. L. *Appl. Phys. Lett.* **2001**, *79*, 2970.
- (9) Hofmann, S.; Ducati, C.; Robertson, J.; Kleinsorge, B. *Appl. Phys. Lett.* **2003**, *83*, 135.
- (10) Christen, H. M.; Poretzky, A. A.; Cui, H.; Belay, K.; Fleming, P. H.; Geohegan, D. B.; Lowndes, D. H. *Nano Lett.* **2004**, *4*, 1939.
- (11) Murakami, Y.; Chiashi, S.; Miyauchi, Y.; Minghui, H.; Ogura, M.; Okubo, T.; Maruyama, S. *Chem. Phys. Lett.* **2004**, *385*, 298.
- (12) Hata, K.; Futaba, D. N.; Mizuno, K.; Namai, T.; Yumura, M.; Iijima, S. *Science* **2004**, *19*, 1362.
- (13) Zhong, G.; Iwasaki, T.; Honda, K.; Furukawa, Y.; Ohdomari, I.; Kawarada, H. *Chem. Vap. Deposition* **2005**, *11*, 127.
- (14) Zhang, G.; Mann, D.; Zhang, L.; Javey, A.; Yenilmez, E.; Wang, Q.; McVittie, J. P.; Nishi, Y.; Gibbons, J.; Dai, H. *Proc. Natl. Acad. Sci. U.S.A.* **2005**, *102*, 16141.
- (15) Xu, Y. Q.; Flor, E.; Kim, M. J.; Hamadani, B.; Schmidt, H.; Smalley, R. E.; Hauge, R. H. *J. Am. Chem. Soc.* **2006**, *128*, 6560.
- (16) Zhang, L.; Tan, Y.; Resasco, D. E. *Chem. Phys. Lett.* **2006**, *422*, 198.
- (17) Zheng, M.; Jagota, A.; Strano, M. S.; Santos, A. P.; Barone, P.; Chou, S. G.; Diner, B. A.; Dresselhaus, M. S.; McLean, R. S.; Onoa, G. B.; Samsonidze, G. G.; Semke, E. D.; Usrey, M.; Walls, D. J. *Science* **2003**, *302*, 1519.
- (18) Krupke, R.; Heinrich, F.; Lohneysen, H.; Kappes, M. M. *Science* **2003**, *301*, 344.
- (19) Wang, Y.; Kim, M. J.; Shan, H.; Kittrell, C.; Fan, H.; Ericson, L. M.; Hwang, W.; Arepalli, S.; Hauge, R. H.; Smalley, R. E. *Nano Lett.* **2005**, *5*, 997.
- (20) Smalley, R. E.; Li, Y.; Moore, V. C.; Price, K.; Colorado, R.; Schmidt, H. K.; Hauge, R. H.; Barron, A. R.; Tour, J. M. *J. Am. Chem. Soc.* **2006**, *128*, 15824.
- (21) Iwasaki, T.; Zhong, G.; Aikawa, T.; Yoshida, T.; Kawarada, H. *J. Phys. Chem. B* **2005**, *109*, 19556.
- (22) Li, X.; Cao, A.; Jung, Y. J.; Vajtai, R.; Ajayan, P. M. *Nano Lett.* **2005**, *5*, 1997.
- (23) Pinault, M.; Pichot, V.; Khodja, H.; Launois, P.; Reynaud, C.; Mayne-L'Hermite, M. *Nano Lett.* **2005**, *5*, 2394.
- (24) Zhu, L.; Xiu, Y.; Hess, D. W.; Wong, C. P. *Nano Lett.* **2005**, *5*, 2641.
- (25) Iwasaki, T.; Maki, T.; Yokoyama, D.; Kumagai, H.; Hashimoto, Y.; Asari, T.; Kawarada, H. *Phys. Stat. Sol. (RRL)* **2008**, *2*, 53.
- (26) Zhong, G.; Iwasaki, T.; Robertson, J.; Kawarada, H. *J. Phys. Chem. B* **2007**, *111*, 1907.
- (27) Zhu, H.; Suenaga, K.; Hashimoto, A.; Urita, K.; Hata, K.; Iijima, S. *Small* **2005**, *1*, 1180.
- (28) Reich, S.; Li, L.; Robertson, J. *Chem. Phys. Lett.* **2006**, *421*, 469.
- (29) Kataura, H.; Kumazawa, Y.; Maniwa, Y.; Umez, I.; Suzuki, S.; Ohtsuka, Y.; Achiba, Y. *Synth. Met.* **1999**, *103*, 2555.
- (30) Telg, H.; Maultzsch, J.; Reich, S.; Hennrich, F.; Thomsen, C. *Phys. Rev. Lett.* **2004**, *93*, 177401.
- (31) Maultzsch, J.; Telg, H.; Reich, S.; Thomsen, C. *Phys. Rev. B* **2005**, *72*, 205438.
- (32) Ding, F.; Bolton, K.; Rosen, A. *J. Phys. Chem. B* **2004**, *108*, 17369.
- (33) Amara, H.; Bichara, C.; Ducastelle, F. *Phys. Rev. B* **2006**, *73*, 113404.
- (34) Raty, J. Y.; Gygi, F.; Galli, G. *Phys. Rev. Lett.* **2005**, *95*, 096103.
- (35) Hofmann, S.; Sharma, R.; Ducati, C.; Du, G.; Mattevi, C.; Cepek, C.; Cantro, M.; Pisana, S.; Parvez, A.; Cervantes-Sodi, F.; Ferrari, A. C.; Dunin-Borkowski, R.; Lizzit, S.; Petaccia, L.; Goldini, A.; Robertson, J. *Nano Lett.* **2007**, *7*, 602.
- (36) Helveg, S.; Lopez-Cartes, C.; Sehested, J.; Hansen, P. L.; Clausen, B. S.; Rostrop-Nielsen, J. R.; Abild-Pedersen, F.; Norskov, J. K. *Nature* **2004**, *427*, 426.
- (37) Maruyama, S. <http://www.photon.t.u-tokyo.ac.jp/~maruyama/wrapping3/wrapping.html>, September 14, 2004.

NL073119F